Responses to comments by reviewer Wolfgang Dorn

We thank Dr. Dorn for his comments, and give our responses in detail below.

General comments:

I am wondering whether this configuration is actually intended for operational use (including CMIP6 simulations) or only an interim solution towards a further improved configuration.
This configuration will not be used for CMIP6 simulations. The Met Office's CMIP6 simulations will be performed with coupled model configurations using the next GSI configuration, which will include the enhancements described in the last paragraph of Section 5 of the present paper.

Specific comments:

(1) Page 2531, lines 11–14: Although the definition of g as a dimensionless function is a correct citation of the paper of Thorndike et al. (1975), I would argue that the statement is incorrect. If g were a dimensionless function, the product g(h)dh would get the unit of a length. Assuming that g(h)dh should actually be a fraction of ice, and given that a fraction is dimensionless by definition, g(h) must have the unit of a reciprocal length. In that case, g(h) can be interpreted as the probability density function that describes the relative probability for the existence of ice with thickness h. The probability itself (that is the fraction) is then given by the integral of g(h) over dh. This would be consistent and would make sense.
We agree with this, and have changed "a dimensionless function" to " a probability density function".
Further, I would not say that g is described by Eq. (1), but that Eq. (1) is the governing equation which describes the evolution of g.
We have changed "g is described by ..." to "The evolution of g(h) with time is described by the governing equation...".

(2) Page 2532, lines 15–18: Does it also mean that the atmospheric surface heat fluxes calculated by JULES are the same for each of the five ice thickness categories? Wouldn't it be another simplification worth being mentioned at this point?
These sentences refer to the ice *layers* in the CICE model, and *not* to the *thickness categories*. However, as mentioned in the conclusions (Section 5), the turbulent fluxes in JULES are indeed calculated as gridbox means (a simplification that will be removed in the next configuration, GSI7.0). We did not state explicitly in the conclusions that the conductive fluxes are calculated separately on each category. We agree with the reviewer that this should be mentioned earlier in the paper than the conclusions section, but think that this would be more appropriate in Section 2.2 (Thermodynamics) than in Section 2.1 (Horizontal and vertical resolution). We have therefore added a paragraph explaining this at the beginning of Section 2.2.

(3) Page 2533, line 2: It would be interesting to know how the fraction of the gridbox area that is covered by snow is determined in the model. The distinction between snow and ice might be just as important as the values chosen for the respective albedos and threshold temperatures.
Our original statement (that the albedos are weighted by the snow-covered fraction of the gridbox) was incorrect. In fact, the total albedo is a weighted combination of the ice and snow albedos, calculated via the "UKMO GCM" parametrisation of Essery et al. (1999) – see the second equation from the top of the right-hand column on p584 of that paper (the equations are not numbered). We have now corrected this error in our paper.

(4) Page 2534, lines 5–9: To my mind, it is not necessary to discuss the enthalpy in the context of the new sea ice configuration. It is rather confusing than helpful. I would cut out these three

sentences.
We have now cut these sentences, as suggested by the reviewer.

(5) Page 2534, lines 22–24: Even without any ridging, the ice area should never be able to exceed the grid-cell area, especially not in case of convergence. Maybe it is meant that the ice does not cover the entire grid cell. This should be clarified.
We agree that this sentence is confusing. What we meant was that if, for example, the area of the grid-cell is A_{GC}, and the area of ice in the grid-cell is A_{ice}, and ice covering area A_{adv} is advected into the grid-cell, where $A_{ice} + A_{adv} > A_{GC}$, then ridging will prevent the (physically impossible) situation arising where the area of ice in the grid-cell is greater than the area of the grid-cell itself. However, as this sentence detracts from the explanation rather than adding to it, we have deleted it.

(6) Page 2535, lines 25–26: The physical argument for increasing the roughness lengths remains unclear. The chosen values seem to me higher than corresponding values derived from measurements and boundary layer theory. Is there any specific reason for this extreme increase, other than the sensitivity study of Rae et al. (2014)?
The roughness lengths quoted here account for form-drag in the MIZ, estimates for which lead to effective roughness lengths of 2 to 4cm. Our value of 10cm is probably above the 3 sigma on the above, but was adopted from a 1970's field observation (original citation lost). However, its adoption in the NWP configuration of the Met Office model leads to an improvement in the simulation of MSLP over that associated with lower (more realistic) values.

Note: More sophisticated parameterizations for the turbulent exchange over sea ice have recently been developed or are still in development (e.g. Lüpkes and Gryanik, 2015, doi:10.1002/2014JD022418). This could be a consideration for future configurations as well.
Indeed, the belated attention to this topic, since the seminal work by Steiner et al. (1998), has led to a number of such formulations. We shall be adapting that of Tsamados et al. (2014) in our next GSI configuration.

(7) Page 2537, line 14: It is unclear to me why increased conductivities lead to reduced basal melt in July and August. The conductive heat flux is negligible during the melting period due to the small temperature difference between top and bottom of the ice. I think this particular conclusion should be explained.
This was explained in Rae et al. (2014), to which we refer in the section concerned. However, for completeness, we have now added the following explanation in the current paper:
"The net melting or growth of Arctic sea ice is the residual of the energy balance, and is extremely sensitive to small changes in the fluxes at the top and bottom of the ice pack (Keen et al., 2013). Rae et al. (2014) found that increased ice and snow conductivities cause an increased upward conductive heat flux through the ice pack in late summer and early autumn, leading to subtle shifts in the energy budget within the ice pack. This results in reduced basal melt in July and August, and increased basal growth in winter, leading to increased thickness, extent and volume."

Technical corrections:

(8) Since the sea ice configuration described in the paper is definite, I would suggest adding the definite article 'the' in the title: Development of the Global Sea Ice 6.0 CICE configuration for the Met Office Global Coupled Model.
Now changed.

(9) Page 2530, line 23: Williams et al. was published in '2015' instead of '2014'.
Now corrected.

(10) Page 2531, line 1: ‘GloSea5’ instead of ‘GloSea4’.
Now corrected.

(11) Page 2532, line 1: The title of the section is ‘Horizontal, temporal and vertical discretisation’, but nothing is said about the temporal discretisation. The word ‘temporal’ could be removed.
Now done.

(12) Page 2532, line 24: ‘parametrisation’ versus ‘parameterisation’ in the next line and in other places.
Now corrected. We are now using 'parametrisation' everywhere.

(13) Page 2532, line 27: ‘(The HadGEM2 Development Team, 2011)’ instead of ‘(HadGEM2 Development Team et al., 2011)’. This team already comprises all authors (‘et al.’ is redundant).
Now corrected.

(14) Page 2533, line 14: ‘Semtner (1976)’ instead of ‘Semtner (1987)’.
Now corrected.

(15) Page 2533, line 17: The symbol f , which is introduced here as the fraction of incident radiation which penetrates the ice pack, has already been used for the rate of change of ice thickness due to thermodynamic growth and melt (page 2531). One of these f s should be replaced by a different symbol.
We have now replaced f for rate of change of ice thickness on p2531 with Φ.

(16) Page 2535, line 25: ‘GSI6.0’ instead of ‘GSI6’.
Now changed.

(17) Page 2535, line 27: calc_Tsfc does not appear in any of the CICE namelists in Appendix A. Or is calc_Tsfc=.false. the default in CICE?
calc_Tsfc=.false. had been omitted from Appendix A in error. We have now included it. We have also deleted year_init, ocn_data_dir, and oceanmixed_file from Appendix A, as they are not relevant for our setup.

(18) Page 2536, line 5: ‘(−1.8 ◦ C)’ instead of ‘(1.8 ◦ C)’. A positive freezing temperature of sea water makes no sense.
Now corrected.

(19) Page 2536, line 10: ‘preprocessor keys’ instead of ‘cpp keys’. It should make no difference whether using cpp or any other preprocessor.
Now changed.

(20) Page 2536, lines 11–12: A reference to Appendix A of similar type has already been given on page 2535. One of them could be dropped.
We have removed the second reference to Appendix A, and retained the first one.

(21) Page 2538, line 3: ‘Labrador Sea’ instead of ‘Labrador sea’.
Now corrected.

(22) Page 2538, line 12: ‘austral’ instead of ‘Austral’.
Now corrected.

(23) Page 2546, lines 11–12: Megann et al. was published in GMD in 2014. The reference to the GMDD version of 2013 is valid but outdated.
We have now updated this to reference the GMD paper.

(24) There is quite a number of papers in the References which are never cited in the discussion paper. These redundant references should be removed.
Several references had indeed survived from an earlier draft of the paper. We have now removed the following from the reference list: Andreas et al. (2010), Calonne et al. (2011), Curry et al. (2001), Dorn et al. (2007), Kim et al. (2006), Lewis (1967), Maykut & Untersteiner (1971), Maykut & McPhee (1995), Miller et al. (2006), Miller et al. (2007), Nakawo & Sinha (1981), Notz & Worster (2009), Pirazzini (2008), Pringle et al. (2006), Pringle et al. (2007), Schwarzacher (1959), Sturm et al. (1997), Uotila et al. (2012), Vancoppenolle et al. (2005), Vancoppenolle et al. (2009), and Wettlaufer (1991). We have not removed the reference to Keen et al. (2013), as we do now cite it as a result of one of the reviewer's other comments.

(25) Page 2550: In the caption of Table 2: 'GC2.0-GSI6.0' instead of 'GC1.0-GSI6.0'.
Now corrected.

(26) In the captions of Table 3 and Figures 2 and 3: Information on the time period of the HadISST and PIOMAS data is missing. They are certainly not 50-year means.
The HadISST and PIOMAS data are means for the period 1995-2004. We have now included this information in the captions of Table 3 and Figures 2 and 3.

(27) The font size in Figure 2 is really close to the lower limit. Maybe the figure can be replotted with a larger font.
We have now increased the font size in this figure.

References:

Essery, R., Martin, E., Douville, H., Fernández, A., and Brun, E.: A comparison of four snow models using observations from an alpine site. Clim.Dyn. 15, 583—593, 1999.

Keen, A.B., Hewitt, H.T., Ridley, J.K.: A case study of a modelled episode of low Arctic sea ice. Clim. Dyn., 41, 5—6, 1229—1244, doi:10.1007/s00382-013-1679-y, 2013.

Rae, J.G.L., Hewitt, H.T., Keen, A.B., Ridley, J.K., Edwards, J.M., and Harris, C.M.: A sensitivity study of the sea ice simulation in HadGEM3, Ocean Modell., 74, 60—76, doi:10.1016/j.ocemod.20, 2014.

Steiner, N., Harder, M., and Lemke, P.: Sea-ice roughness and drag coefficients in a dynamic-thermodynamic sea-ice model for the Arctic. Tellus A, 51, 5, 964-978, doi:10.1034/j.1600-0870.1999.00029.x, 1998.

Tsamados, M., Feltham, D.L., Schröder, D., Flocco, D., Farrell, S.L., Kurtz, N., Laxon, S.W., and Bacon, S.: Impact of Variable Atmospheric and Oceanic Form Drag on Simulations of Arctic Sea Ice. J.Phys.Oceanog. 44, 5, 1329-1353, doi:10.1175/JPO-D-13-0215.1, 2014.

Responses to comments by reviewer David Bailey

We thank Dr. Bailey for his comments, and give our responses below.

This manuscript describes an update to the Met Office Global Coupled Model. The CICE model itself remains the same, but some of the internal parameters have changed. These do have the desirable effect of improving the Arctic Sea Ice simulation, but overall the Antarctic sea ice simulation is substantially degraded. While I agree that this is due to the change in the ocean model resolution, I believe that the experiments described here are fundamentally flawed and not worthy of publication at this point.

My main issue is that the nominal resolution of 0.25 degrees is not eddy-resolving as the authors suggest. A recent paper by Griffies et al. 2015 clearly outlines that a resolution of 0.25-degrees with no Gent-McWilliams or similar eddy parameterization leads to a substantially larger drift in the global ocean temperature (see their Figure 2). The results at 0.1-degree are closer overall in these metrics when compared to a 1-degree ocean simulation with GM. New simulations should be performed either at 0.25 degrees with a GM-like parameterization or at 0.1-degree to begin to assess the changes in the CICE model parameters.
The resolution of 0.25 degrees is, as the reviewer points out, not eddy-*resolving*. However, it is considered to be eddy-*permitting*, and it is this term that we use in the paper. The results presented by Griffies et al. (2015) do indeed indicate that the parameterisation of mesoscale eddies in the GFDL model at 0.25 degrees resolution requires additional vertical mixing. In NEMO at ORCA025 we use a latitude-dependent viscosity and isopycnal diffusion which result in similar SST biases for this $^{1}/_{4}$ degree model as we see in our $^{1}/_{12}$-degree NEMO configuration. In addition we do not observe the cool bias at depth as in the GFDL model. Consequently we do not think the issues described for the GFDL model are related to our biases. The Southern Ocean warm bias in NEMO at ORCA025 is solely related to the cloud-related surface short wave bias. We therefore do not expect that running at 0.1 degree, as suggested by the reviewer, would alter our results.

Also, the changes to the CICE parameters should be systematically evaluated to determine which of these has the largest effect in improving the Arctic sea ice. Also, once the ocean simulation has been improved, a similar analysis of the impacts of these on the Antarctic sea ice is needed.
We have published such a study previously (Rae et al., 2014). We mentioned this briefly at the beginning of Section 4 of the submitted manuscript: "In this section, the differences between GSI6.0 and GSI4.0 will be discussed, and put in the context of the findings of Rae et al. (2014)". However, we have now expanded this by adding the following summary of that paper: "That study found that snow albedo, and snow and ice thermal conductivities, had the largest effect on Arctic sea ice, and that the winter Arctic ice extent was strongly influenced by a move to higher ice-ocean model resolution, through its effect on sea-surface temperatures in the Labrador Sea. Rae et al (2014) also found that in the Antarctic, the effects of changing atmospheric and oceanic forcing generally dominated over those of changing sea ice parameters, and that the Antarctic sea ice simulation in the model was also strongly sensitive to increased ice-ocean resolution."

Reference:

Rae, J.G.L., Hewitt, H.T., Keen, A.B., Ridley, J.K., Edwards, J.M., and Harris, C.M.: A sensitivity study of the sea ice simulation in HadGEM3, Ocean Modell., 74, 60–76, doi:10.1016/j.ocemod.20, 2014 .

Manuscript prepared for Geosci. Model Dev. Discuss.
with version 3.5 of the LaTeX class copernicus_discussions.cls.
Date: 30 June 2015

Development of the Global Sea Ice 6.0 CICE configuration for the Met Office Global Coupled Model

J.G.L. Rae[1], H.T. Hewitt[1], A.B. Keen[1], J.K. Ridley[1], A.E. West[1], C.M. Harris[1], E.C. Hunke[2], and D.N. Walters[1]

[1]Met Office Hadley Centre, FitzRoy Road, Exeter, EX1 3PB, United Kingdom
[2]MS-B216, Los Alamos National Laboratory, Los Alamos, NM 87545, United States

Correspondence to: J.G.L. Rae (jamie.rae@metoffice.gov.uk)

Abstract

The new sea ice configuration GSI6.0, used in the Met Office global coupled configuration GC2.0, is described and the sea ice extent, thickness and volume are compared with the previous configuration and with observationally-based datasets. In the Arctic, the sea ice is thicker in all seasons than in the previous configuration, and there is now better agreement of the modelled concentration and extent with the HadISST dataset. In the Antarctic, a warm bias in the ocean model has been exacerbated at the higher resolution of GC2.0, leading to a large reduction in ice extent and volume; further work is required to rectify this in future configurations.

1 Introduction

Within the Met Office's model development framework, there are four model components: atmosphere, using the Met Office Unified Model (MetUM, see Cullen and Davies, 1991; Davies et al., 2005); land surface, using the Joint UK Land Environment Simulator (JULES, see Best et al., 2011); ocean, using the Nucleus for European Modelling of the Ocean (NEMO, see Madec, 2008); and sea ice, using the Los Alamos Sea Ice Model, CICE (Hunke and Lipscomb, 2010). The UM and JULES run together as one executable, as do NEMO and CICE. UM-JULES and NEMO-CICE communicate via the OASIS coupler (Valcke, 2006).

The Met Office configurations of each component are known as Global Atmosphere (GA), Global Land (GL), Global Ocean (GO) and Global Sea Ice (GSI), and the combined system is known as the Global Coupled (GC) configuration. These terms are suffixed by a version number (e.g., "GA6.0", "GC2.0"). The second coupled configuration, GC2.0 (Williams et al., 2015), includes GA6.0 and GL6.0 (both described by Walters et al., 2014), GO5.0 (Megann et al., 2014) and GSI6.0. GC2.0 will be used on a range of spatial scales (regional and global), and on a range of temporal scales, from ocean forecasting (FOAM; see Blockley et al., 2014), through seasonal and decadal prediction (GloSea5; see MacLachlan et al., 2014), to centennial-scale climate projections (HadGEM3; see Hewitt et al., 2011). In the present paper, we consider only the climate configuration, HadGEM3.

Sea ice is a key component of the earth system because of its role in the energy balance of the polar regions. An accurate simulation of sea ice is therefore essential in fully-coupled atmosphere-ocean-ice models run on any timescale. Here, we describe the model setup and parametrisations used in GSI6.0 as part of GC2.0, and discuss how the change from the previous configuration (GSI4.0) to GSI6.0 has affected simulated sea ice extent, thickness and volume.

2 Description of GSI6.0

Thorndike et al. (1975) defined the ice thickness distribution (ITD), g, as a probability density function such that $g(h)dh$ is the fraction of ice in thickness range h to $h+dh$. The evolution of $g(h)$ with time is described by the governing equation:

$$\frac{\partial g}{\partial t} = -\nabla \cdot (\mathbf{v}g) - \frac{\partial(\Phi g)}{\partial h} + \psi, \quad (1)$$

where $\nabla \cdot (\mathbf{v}g)$ is the rate of change of g due to dynamical processes ($\mathbf{v}$ is the ice velocity), Φ is the rate of change of ice thickness due to thermodynamic growth and melt, and ψ gives the contribution from mechanical redistribution (ridging). A full explanation is given by Thorndike et al. (1975). The CICE sea ice model solves this equation to determine the evolution of g in time and space. Full details of the model are available in the CICE user manual (Hunke and Lipscomb, 2010); here we summarise the main features of the model used in GSI, and detail the specific settings and choices for the previous configuration (GSI4.0) and the new configuration (GSI6.0). Much of the basic model description is provided in Appendix D of Hewitt et al. (2011), but it is reproduced here for completeness.

2.1 Horizontal and vertical discretisation

The GSI configurations discussed here use code revision 430 of CICE version 4.1, which allows a tripolar grid to be employed. These configurations use essentially the same family of ORCA grids as the NEMO model (see Appendix C of Hewitt et al., 2011), although CICE uses an Arakawa B grid rather than a C grid and so the CICE velocity grid points are not coincident with the NEMO velocity points. The grid and land-mask definitions required by CICE are read in directly from a file, as are the initial conditions. The sub-grid-scale ITD is modelled by dividing the ice pack at each grid point into a number of thickness categories. GSI uses five categories, plus an open-water category, which has been shown to be sufficient for climate modelling (Bitz et al., 2001). The lower bounds for the five thickness categories are 0, 0.6, 1.4, 2.4 and 3.6 m. GSI uses the zero-layer thermodynamic model of Semtner (1976) to calculate the growth and melt of the sea ice, with one layer of snow and one layer of ice in the vertical. This is not the standard scheme implemented in CICE, which has a multilayer ice model (Bitz and Lipscomb, 1999). It was not possible to use the CICE multilayer thermodynamics in GSI because the surface temperature at sea ice points, and the conductive heat flux into the ice, are currently calculated by the JULES land-surface model (which also models surface exchange over the ocean and sea ice). This would not be consistent with the CICE multilayer thermodynamics scheme, which calculates these quantities itself, so for GSI CICE has been adapted to use the zero-layer surface fluxes received from the UM atmosphere.

2.2 Thermodynamics

As discussed in the previous section, the GSI configurations use five ice thickness categories in the CICE model. While the conductive heat fluxes through the ice are calculated in the JULES land-surface model on these five categories, the ice albedo and the turbulent (latent and sensible) heat fluxes are currently calculated as gridbox means.

The sea ice albedo is calculated as a function of temperature and snow cover, including a parametrisation to represent the impact of melt ponds, and – in the zero-layer model – a parametrisation to account for the effects of scattering. This is the same scheme used in HadGEM1 (McLaren et al., 2006), HadGEM2 (HadGEM2 Development Team, 2011) and HadGEM3 (Hewitt et al., 2011). The total albedo is calculated from the ice albedo α_i and the snow albedo α_s, following the parametrisation of Essery et al. (1999),

$$\alpha_{tot} = \alpha_i + (\alpha_i - \alpha_s)(1 - \exp(-0.2S)),$$

where S is the mass of snow per unit area.

Bare ice albedo α_b is set as a single value. The ice albedo α_i is then calculated by applying corrections to α_b to account for the presence of melt ponds, and for scattering within the ice pack. Melt ponds are assumed to form on bare ice when the ice temperature reaches a threshold temperature T_p. As the temperature increases between T_p and the melting temperature T_m, melt ponds are assumed to reduce the ice albedo α_i linearly,

$$\alpha_i = \begin{cases} \alpha_b & \text{if } T < T_p \\ \alpha_b + \frac{\mathrm{d}\alpha_i}{\mathrm{d}T}(T - T_p) & \text{if} T_p \leq T \leq T_m \end{cases},$$

where T_m is fixed at 0°C for all simulations while the values of T_p and $\frac{\mathrm{d}\alpha_i}{\mathrm{d}T}$ can be set as parameters for each simulation.

Because the ice model configuration uses a zero-layer approximation, an additional parametrisation is required to account for the effects of internal scattering (e.g. from brine pockets) on the albedo. Following the suggestion of Semtner (1976), a correction $\Delta\alpha_i$ is applied to the ice albedo,

$$\Delta\alpha_i = f\beta(1-\alpha_i),$$

where f is the fraction of incident radiation which penetrates the ice pack, and β is an attenuation factor to take account of backscatter.

Snow albedo α_s is assumed to vary linearly with temperature between that of cold, dry snow (α_c) at a threshold temperature T_c, and that of melting snow (α_m) at the melting point, T_m,

$$\alpha_s = \begin{cases} \alpha_c & \text{if } T < T_c \\ \alpha_c + \frac{\alpha_m - \alpha_c}{T_m - T_c}(T - T_c) & \text{if } T_c \leq T \leq T_m \end{cases},$$

where T_m is fixed at 0°C while T_c, α_c and α_m can be varied.

As in HadGEM1, the sea-ice surface temperature and the atmosphere-to-ice fluxes are calculated in JULES (see McLaren et al., 2006, for details). Within CICE these fluxes (downward latent heat flux, surface sensible heat flux, and conductive flux through the ice), along with the ocean-ice heat flux (McPhee, 1992), determine the rate at which the ice grows or melts in each thickness category. The calculated thermodynamic growth or melt rates are then used in the linear remapping scheme of Lipscomb (2001) to exchange the ice between thickness categories.

2.3 Dynamics and ridging

The ice velocities are calculated by solving the 2-D momentum equation for the force balance per unit area in the ice pack (Hibler, 1979), including terms for wind stress, ocean stress, internal ice stress, and stresses due to Coriolis effects. The internal ice stress is calculated using the elastic viscous plastic (EVP) scheme (Hunke and Dukowicz, 2002), which assumes the ice has a viscous plastic rheology, and incorporates an elastic wave modification to improve the computational efficiency. The GSI configurations use the Rothrock et al. (1975) formulation for ice strength. The sea ice is advected using the CICE incremental remapping scheme (Lipscomb and Hunke, 2004). The mechanical redistribution (or ridging) scheme in CICE converts thinner ice to thicker ice and open water, and is applied after the advection of ice. The scheme is based on work by Thorndike et al. (1975), Hibler (1980), Flato and Hibler (1995), and Rothrock et al. (1975). It favours the closing of open water and ridging of the thinnest ice over the ridging of thicker ice. In GSI the ridging participation function suggested by Lipscomb et al. (2007) is used. The ridged ice is then distributed between thickness categories assuming an exponential ITD (Lipscomb et al., 2007).

2.4 CICE settings used for GSI6.0

Rae et al. (2014) investigated the sensitivity of Arctic and Antarctic sea ice extent, thickness and volume in GSI4.0 to changes in several sea ice physical parameters, as well as to changes in the resolutions of the atmosphere and ocean models. By testing each of these sensitivities in isolation, they identified an optimum set of sea ice parameters for use in the Met Office coupled configuration. They found the Arctic sea ice to be most sensitive to changes in the albedos and thermal conductivities of ice and snow, while the Antarctic sea ice was most sensitive to changes in ice salinity, atmospheric and oceanic forcing, and ice-ocean model resolution.

This forms the basis for the set of parameters used in GSI6.0, with some adjustments to account for the effect of changes in the atmosphere model made at the same time (see Walters et al., 2014). Parameter values are given in Table 1. The CICE namelist used in GSI6.0, which has been edited to detail the scientific options only, is given in Appendix A. The albedo parameters α_{m}, f and β, were set in such a way as to increase the surface albedo, thereby reducing summer melt; the other albedo parameters were left unchanged. The values of the thermal conductivities of ice and snow, κ_{ice} and κ_{snow}, were chosen to increase the heat flux through the ice in autumn and winter, thereby increasing ice growth. The ice salinity, S, was increased, because Rae et al. (2014) found that this led to greater Antarctic ice growth due to a colder ocean mixed layer through the effect of salinity on ocean mixing. Rae et al. (2014) found the Arctic and Antarctic sea ice extent and volume to be relatively insensitive to the value of the ridging parameter μ_{rdg} (Hunke, 2010); however, the value was reduced from 4 m$^{1/2}$ to 3 m$^{1/2}$ as this is now the recommended value. The roughness lengths of pack ice and the marginal ice zone, z_0(ice) and z_0(MIZ), previously had different values in the climate and Numerical Weather Prediction (NWP) configurations of the model. In GSI6.0, the values in the climate configurartion have been increased to make them consistent with those in the NWP configuration.

For coupling with the UM atmosphere, `heat_capacity` and `calc_Tsfc` are both set to `false`. This means that zero-layer thermodynamics are used and that CICE does not calculate any surface fluxes or the surface ice temperature. Note that setting `calc_Tsfc` to `false` also means that the albedo settings in the CICE namelist are irrelevant as the albedo is not calculated by CICE. Wind stresses are passed from the UM atmosphere rather than being calculated in CICE, so `calc_strair` is set to `false`. A constant value for the freezing point of sea water is used ($-1.8°$C), by setting

`Tfrzpt='constant'`. This is required for consistency with the UM atmosphere-ice thermodynamics. The variable `ns_boundary_type` is set to `tripole` for the ORCA1 grid (i.e. in GSI4.0), indicating a tripolar grid with the "north fold" occurring along velocity points. The alternative setting `tripoleT` is used for the ORCA025 grid (i.e. in GSI6.0) where the north fold occurs along temperature points. The CICE preprocessor keys used in HadGEM3 at GC2.0 are shown in Table 2.

3 Experimental setup

We compare sea ice simulations from GSI6.0 (within GC2.0) with those from the previous configuration, GSI4.0 (within an earlier configuration of the coupled model). Both simulations were performed with a fully-coupled configuration of the Met Office's modelling system. The atmosphere and land-surface models were run on an N96 grid (equivalent to a resolution of 1.875° in longitude and 1.25° in latitude); the ocean and sea-ice models were on an ORCA1 grid (nominal 1° resolution) for GSI4.0, and an ORCA025 grid (nominal 0.25° resolution) for GSI6.0. The model setups and parameter values used are given in Table 1. Both simulations used initial conditions, greenhouse gas concentrations, and emissions of aerosols and their precursors appropriate for the present day (equivalent to year 2000). In both cases, we consider 50 years of output following an 80-year spin-up.

4 Model evaluation

In GSI4.0, the Arctic ice volume (Fig. 2c; Table 3) was too low relative to that from the PanArctic IceOcean Modeling and Assimilation System (PIOMAS, see Schweiger et al., 2011), a coupled ice-ocean model that includes assimilation of observations. The findings of Rae et al. (2014), and the poor agreement of GSI4.0 Arctic sea ice with observational datasets, informed the choice of parameter values for GSI6.0 (see Table 1).

In this section, the differences between GSI6.0 and GSI4.0 will be discussed, and put in the context of the findings of Rae et al. (2014). That study found that snow albedo, and snow and ice thermal conductivities, had the largest effect on Arctic sea ice, and that the winter Arctic ice extent was strongly influenced by a move to higher ice-ocean model resolution, through its effect on sea-surface temperatures in the Labrador Sea. Rae et al. (2014) also found that in the Antarctic, the effects of changing atmospheric and oceanic forcing generally dominated over those of changing sea ice parameters, and that the Antarctic sea ice simulation in the model was also strongly sensitive to increased ice-ocean resolution.

4.1 Arctic

In GSI6.0, we see thickening of the Arctic ice pack at the end of winter relative to GSI4.0 (Fig. 1a,b), resulting in improved agreement with observations (see Fig. 1 of Laxon et al., 2013). The net melting or growth of Arctic sea ice is the residual of the energy balance, and is extremely sensitive to small changes in the fluxes at the top and bottom of the ice pack (Keen et al., 2013). Rae et al. (2014) found that increased ice and snow thermal conductivities cause an increased upward conductive heat flux through the ice pack in late summer and early autumn, leading to subtle shifts in the energy budget within the ice pack. This results in reduced basal melt in July and August, and increased basal growth in winter, leading to increased thickness, extent and volume.

We also see an increase in summer ice extent, thickness and volume in GSI6.0 compared to GSI4.0 (Figs. 1c,d, 3d,e, 2a, 2c; Table 3). This mirrors the behaviour seen by Rae et al. (2014) with increased ice and snow thermal conductivities, where the increased ice thickness seen in winter persisted through the following melt season. In addition to this, Rae et al. (2014) also found that in the Arctic increased snow albedo led to reduced surface melt in summer, and thus to increased summer ice extent, thickness and volume. It is likely that similar effects are occurring here in GSI6.0. The summer ice concentration and extent are now more in agreement with the HadISST dataset of

Rayner et al. (2003) (Figs. 3f, 2a), and the agreement of the volume with PIOMAS has also improved (Fig. 2c; Table 3).

In winter, there are also overall improvements in the total extent relative to HadISST (Fig. 2a; Table 3), largely due to reduced ice cover in the Labrador Sea (Fig. 3a,b,c). The investigations of Rae et al. (2014) suggest that this is attributable to the increased ice-ocean model resolution. They found that the increased resolution led to warmer sea surface temperatures in the Labrador Sea, leading in turn to a reduced sea ice concentration there, and thus to a lower total Arctic winter sea ice extent. Despite this reduced winter ice extent, the increased ice thickness has led to an increased ice volume, with the result that it is now more in agreement with that from PIOMAS (Fig. 2c; Table 3).

4.2 Antarctic

The GC simulations have been found to display a warm bias in sea-surface temperatures (SST) in the Southern Ocean (Megann et al., 2014), due to a positive bias in downward heat flux from the atmosphere into the ocean (Williams et al., 2015). In GSI4.0, this led to a low Antarctic sea ice extent in austral summer, although the winter ice extent compared favourably with HadISST (Fig. 2b; Table 3).

Rae et al. (2014) found that the Antarctic ice extent and volume were generally insensitive to perturbations in the ice physics parameters (other than salinity), but that the effects of the warm SST bias were exacerbated at higher ice-ocean resolution. They attributed this to the removal of the Gent-McWilliams eddy parametrisation at the eddy-permitting resolution of ORCA025. It is thought that this parametrisation helps to mask the warm bias at lower resolution, but that its removal in the higher-resolution runs leads to increased southward heat transport in the ocean.

As discussed in Sect. 3, GSI6.0 is run at the higher resolution of ORCA025 (see Table 1). The exacerbation of the warm bias in the Southern Ocean therefore has an impact on the Antarctic sea ice in GSI6.0, and there is a substantial reduction in ice extent and volume in all seasons (Figs. 2b,d; Table 3). Thus, while the transition from

GSI4.0 to GSI6.0 leads to some improvements in the Arctic, the same is not true in the Antarctic. Work is ongoing to reduce the warm bias in the Southern Ocean, and it is anticipated that this will lead to improved simulations of Antarctic sea ice in future configurations.

5 Conclusions

We have described and evaluated the new Global Sea Ice configuration, GSI6.0, run within the Met Office Global Coupled model configuration GC2.0. The choice of parameters for GSI6.0 was informed by the work of Rae et al. (2014), who conducted an extensive sea ice parameter sensitivity study within the Met Office coupled modelling system and in addition isolated the impact of ice physics changes from that of forcing and resolution changes. In the new configurations, the values of several sea ice parameters have been changed, and the ice-ocean model resolution has been increased from ORCA1 (nominal 1° resolution) to ORCA025 (nominal 0.25° resolution). This has resulted in thicker Arctic ice in all seasons, and Arctic ice concentration and extent that are in better agreement with the HadISST observational dataset (Rayner et al., 2003). In the Antarctic, the higher ice-ocean model resolution has resulted in the exacerbation of an existing warm bias in the Southern Ocean. This has in turn led to a large reduction in ice extent and volume. Rectification of this bias will require further development work on atmosphere-ocean heat transfer in the coupled model.

While the sea ice simulation in GSI6.0 represents an improvement over that in GSI4.0 – at least in the Arctic – there are still several areas in which there is potential for further model enhancement. First, while the GSI configurations use five ice thickness categories in the CICE model,and the conductive heat fluxes through the ice are calculated on these categories as mentioned in Sect. 2.2, the albedo and the surface latent and sensible heat fluxes are calculated in the JULES land-surface scheme as gridbox means. In the next configuration, these calculations will be performed on all five thickness categories. Second, the sea ice surface albedo scheme used in GSI4.0

and GSI6.0 is the same broadband scheme used in HadGEM1 (McLaren et al., 2006). The next configuration will include separate calculations for four radiation bands – direct and diffuse radiation for both visible and near-infrared bands – as well as for each ice thickness category. It is anticipated that future configurations will also include an explicit representation of the effect of melt ponds on surface albedo. As mentioned in Section 2.4, GSI currently uses a fixed reference value of $-1.8°$C for the freezing temperature of sea water. In future configurations, this freezing temperature will be calculated as a function of ocean salinity. Finally, as mentioned in Section 2.1, the current GSI configurations use the zero-layer thermodynamics of Semtner (1976, 1987), rather than the full multi-layer CICE scheme. Planned modifications to CICE, the UM, and JULES will enable the CICE multilayer model to be used with the UM atmosphere in the future.

Appendix A CICE namelist used in GSI6.0

```
&setup_nml
    days_per_year  = 360
  , istep0         = 0
  , dt             = 1350.0
  , ndyn_dt        = 1
/

&grid_nml
    grid_format  = 'nc'
  , grid_type    = 'tripole'
  , kcatbound    = 1
/

&domain_nml
```

```
    nprocs            = 368
  , processor_shape   = 'square-pop'
  , distribution_type = 'cartesian'
  , distribution_wght = 'block'
  , ew_boundary_type  = 'cyclic'
  , ns_boundary_type  = 'tripoleT'
/

&ice_nml
    kitd            = 1
  , kdyn            = 1
  , ndte            = 120
  , kstrength       = 1
  , krdg_partic     = 1
  , krdg_redist     = 1
  , mu_rdg          = 3.0
  , advection       = 'remap'
  , heat_capacity   = .false.
  , conduct         = 'MU71'
  , atmbndy         = 'default'
  , calc_strair     = .false.
  , calc_Tsfc       = .false.
  , precip_units    = 'mks'
  , Tfrzpt          = 'constant'
  , ustar_min       = 5.0e-4
  , update_ocn_f    = .true.
  , oceanmixed_ice  = .false.
  , ocn_data_format = 'nc'
  , sss_data_type   = 'default'
```

```
  , sst_data_type   = 'default'
  , restore_sst     = .false.
  , trestore        =  0
  , restore_ice     = .false.
/
```

Appendix Code availability

The MetUM is available for use under licence. A number of research organisations and national meteorological services use the MetUM in collaboration with the Met Office to undertake basic atmospheric process research, produce forecasts, develop the MetUM code and build and evaluate Earth system models. For further information on how to apply for a licence see http: //www.metoffice.gov.uk/research/collaboration/um-collaboration.

JULES is available under licence free of charge. For further information on how to gain permission to use JULES for research purposes see https://jules.jchmr.org/software-and-documentation

The model code for NEMO v3.4 is available from the NEMO website (www.nemo-ocean.eu). On registering, individuals can access the code using the open source subversion software (http://subversion.apache.org/).

The model code for CICE is freely available from the United States Los Alamos National Laboratory (http://oceans11.lanl.gov/trac/CICE/wiki/SourceCode), again using subversion.

The versions and revisions of each model used in this paper are given in 1. A number of branches are applied to these codes. Please contact the authors for more information on these branches and how to obtain them.

Acknowledgements. We are grateful to Alison McLaren and Ed Blockley for useful comments on earlier drafts of the manuscript. This work was supported by the Joint DECC/Defra Met

Office Hadley Centre Climate Programme (GA01101).

References

Best, M.J., Pryor, M., Clark, D.B., Rooney, G.G., Essery, R.L.H., Ménard, C.B., Edwards, J.M., Hendry, M.A., Porson, A., Gedney, N., Mercado, L.M., Sitch, S., Blyth, E., Boucher, O., Cox, P.M., Grimmond, C.S.B., and Harding, R.J.: The Joint UK Land Environment Simulator (JULES), model description – Part 1: Energy and water fluxes, Geosci.Model Dev., 4, 1–23, 2011.

Bitz, C., Holland, M., Weaver, A., and Eby, M.: Simulating the ice-thickness distribution in a coupled climate model, J.Geophys.Res., 106, 2441-2463, 2001.

Bitz, C.M., and Lipscomb, W.H.: An energy-conserving thermodynamic model of sea ice, J.Geophys.Res., 104 (C7), 15669–15677, 1999.

Blockley, E. W., Martin, M. J., McLaren, A. J., Ryan, A. G., Waters, J., Lea, D. J., Mirouze, I., Peterson, K. A., Sellar, A., and Storkey, D.: Recent development of the Met Office operational ocean forecasting system: an overview and assessment of the new Global FOAM forecasts, Geosci. Model Dev., 7, 2613-2638, doi:10.5194/gmd-7-2613-2014, 2014.

Cullen, M.J.P., Davies, T., 1991. A conservative split-explicit integration scheme with fourth-order horizontal advection. Q. J. Roy. Meteorol. Soc. 117, 993–1002.

Davies, T., Cullen, M.J.P., Malcolm, A.J., Mawson, M.H., Staniforth, A., White, A.A., and Wood, N.: A new dynamical core for the Met Office's global and regional modelling of the atmosphere, Q.J.Roy.Meteor.Soc., 131, 1759–1782, 2005.

Essery, R., Martin, E., Douville, H., Fernández, A., and Brun, E.: A comparison of four snow models using observations from an alpine site. Clim.Dyn. 15, 583–593, 1999.

Flato, G. and Hibler, W.: Ridging and strength in modeling the thickness distribution of Arctic sea ice, J.Geophys.Res., 100, 18611-18626, 1995.

HadGEM2 Development Team: Martin, G.M., Bellouin, N., Collins, W.J., Culverwell, I.D., Halloran, P.R., Hardiman, S.C., Hinton, T.J., Jones, C.D., McDonald, R.E., McLaren, A.J., O'Connor, F.M., Roberts, M.J., Rodriguez, J.M., Woodward, S., Best, M.J., Brooks, M.E., Brown, A.R., Butchart, N., Dearden, C., Derbyshire, S.H., Dharssi, I., Doutriaux-Boucher, M., Edwards, J.M., Falloon, P.D., Gedney, N., Gray, L.J., Hewitt, H.T., Hobson, M., Huddleston, M.R., Hughes, J., Ineson, S., Ingram, W.J., James, P.M., Johns, T.C., Johnson, C.E., Jones, A., Jones, C.P., Joshi, M.M., Keen, A.B., Liddicoat, S., Lock, A.P., Maidens, A.V., Manners, J.C., Milton, S.F., Rae, J.G.L., Ridley, J.K., Sellar, A., Senior, C.A., Totterdell, I.J., Verhoef, A., Vidale, P.L., and Wiltshire, A.: The HadGEM2 family of Met Office Unified Model climate configurations, Geosci. Model Dev., 4 (3), 723–757, doi:10.5194/gmd-4-723-2011, 2011.

Hewitt, H. T., Copsey, D., Culverwell, I. D., Harris, C. M., Hill, R. S. R., Keen, A. B., McLaren, A. J., and Hunke, E. C.: Design and implementation of the infrastructure of HadGEM3: the next-generation Met Office climate modelling system, Geosci. Model Dev., 4, 223–253, doi:10.5194/gmd-4-223-2011, 2011.

Hibler, W.: A dynamical thermodynamic sea ice model, J.Phys.Oceanogr., 9, 817-846, 1979.

Hibler, W.: Modeling a variable thickness sea ice cover, Mon. Weather Rev., 108, 1943-1973, 1980.

Hunke, E. C.: Thickness sensitivities in the CICE sea ice model, Ocean Modell., 34, 137–149,doi:10.1016/j.ocemod.2010.05.004, 2010.

Hunke, E. C. and Dukowicz, J. K.: The Elastic-Viscous-Plastic Sea Ice Dynamics Model in General Orthogonal Curvilinear Coordinates on a SphereIncorporation of Metric Terms, Mon. Weather Rev., 130, 1848-1865, 2002.

Hunke, E.C., and Lipscomb, W.H.: CICE: the Los Alamos sea ice model documentation and software users' manual, Version 4.1, LA-CC-06-012, Los Alamos National Laboratory, N.M., 2010.

Keen, A.B., Hewitt, H.T., Ridley, J.K.: A case study of a modelled episode of low Arctic sea ice. Clim. Dyn.,41, 5–6, 1229–1244, doi:10.1007/s00382-013-1679-y, 2013.

Laxon, S. W., Giles, K. A., Ridout, A. L., Wingham, D. J., Willatt, R., Cullen, R., Kwok, R., Schweiger, A., Zhang, J. L., Haas, C., Hendricks, S., Krishfield, R., Kurtz, N., Farrell, S., and Davidson, M: CryoSat-2 estimates of Arctic sea ice thickness and volume, Geophys. Res. Lett., 40, 4, 732–737, doi:10.1002/grl.50193, 2013.

Lipscomb, W.: Remapping the thickness distribution in sea ice models, J.Geophys.Res., 106, 13989-14000, 2001.

Lipscomb, W.H. and Hunke, E.H.: Modeling sea ice transport using incremental remapping, Mon. Weather Rev., 132, 1341-1354, 2004.

Lipscomb, W.H., Hunke, E.C., Maslowski, W., and J. Jakacki: Ridging, strength, and stability in high-resolution sea ice models, J.Geophys.Res., 112, C03S91, doi:10.1029/2005JC003355, 2007.

Madec, G.: NEMO Ocean Engine, Note du Pole de Modélisation, Institut Pierre-Simon Laplace (IPSL), France, No 27, ISSN No 1288-1619, 2008.

MacLachlan, C., Arribas, A., Peterson, K. A., Maidens, A., Fereday, D., Scaife, A. A., Gordon, M., Vellinga, M., Williams, A., Comer, R. E., Camp, J., Xavier, P., and Madec, G.: Global Seasonal Forecast System version 5 (GloSea5): a high resolution seasonal forecast system, Q. J. Roy. Meteor. Soc., doi:10.1002/qj.2396, 2014.

McLaren, A.J., Banks, H.T., Durman, C.F., Gregory, J.M., Johns, T.C., Keen, A.B., Ridley, J.K., Roberts, M.J., Lipscomb, W.H., Connolley, W.M., and Laxon, S.W.: Evaluation of the sea ice simulation in a new coupled atmosphere-ocean climate model (HadGEM1), J.Geophys.Res., 111, C12014, doi:10.1029/2005JC003033, 2006.

McPhee, M.G.: Turbulent heat flux in the upper ocean under sea ice, J.Geophys.Res., 97 (C4), 5365–5379, 1992.

Megann, A., Storkey, D., Aksenov, Y., Alderson, S., Calvert, D., Graham, T., Hyder, P., Siddorn, J., and Sinha , B.: GO5.0: the joint NERC-Met Office NEMO global ocean model for use in coupled and forced applications, Geosci. Model Dev, 7,1069–1092, doi:10.5194/gmd-7-1069-2014, 2014.

Rae, J.G.L., Hewitt, H.T., Keen, A.B., Ridley, J.K., Edwards, J.M., and Harris, C.M.: A sensitivity study of the sea ice simulation in HadGEM3, Ocean Modell., 74, 60–76, doi:10.1016/j.ocemod.20, 2014.

Rayner, N.A., Parker, D.E., Horton, E.B., Folland, C.K., Alexander, L.V., Rowell, D.P., Kent, E.C., Kaplan, A.: Global analyses of sea surface temperature, sea ice, and night marine air temperature since the late nineteenth century, J.Geophys.Res., 108 (D14), 4407, doi:10.1029/2002JD002670, 2003.

Rothrock, D.: The energetics of the plastic deformation of pack ice by ridging, J.Geophys.Res., 80, 4514-4519, 1975.

Schweiger, A., Lindsay, R., Zhang, J., Steele, M., Stern, H., and Kwok, R.: Uncertainty in modeled Arctic sea ice volume, J.Geophys.Res., 116, C00D06, doi:10.1029/2011JC007084, 2011.

Semtner A.J.: A model for the thermodynamic growth of sea ice in numerical investigations of climate, J.Phys.Oceanog., 6, 379–389, 1976.

Semtner A.J.: A numerical study of sea ice and ocean circulation in the Arctic, J.Phys.Oceanog., 17, 1077–1099, 1987.

Thorndike, A., Rothrock,, D., Maykut, G., and Colony, R.: The thickness distribution of sea ice,

J.Geophys.Res., 80, 4501-4513, 1975.
Valcke, S.: OASIS3 User Guide (prism_2-5). PRISM Support Initiative No 3, 68 pp., 2006.
Walters, D.N., et al.: The Met Office Unified Model Global Atmosphere 6.0/6.1 and JULES Global Land 6.0/6.1 configurations, Geosci. Model Dev. Discuss., in preparation.
Williams, K.D., Harris, C.M., Bodas-Salcedo, A., Camp, J., Comer, R.E., Copsey, D., Fereday, D., Graham, T., Hill, R., Hinton, T., Hyder, P., Ineson, S., Masato, G., Milton, S.F., Roberts, M.J., Rowell, D.P., Sanchez, C., Shelly, A., Sinha, B., Walters, D.N., West, A., Woollings, T., and Xavier, P.K.: The Met Office Global Coupled model 2.0 (GC2) configuration, Geosci. Model Dev., 8, 1509-1524, doi:10.5194/gmd-8-1509-2015, 2015.

Table 1. Model setup and values of sea ice parameters in GSI4.0 and GSI6.0 simulations

		GSI4.0	GSI6.0
CICE revision number		430	430
Atmosphere configuration (UM version)		GA4.0 (UM8.2)	GA5.0 (UM8.5)
Land surface configuration (UM version)		GL4.0 (UM8.2)	GL5.0 (UM8.5)
Ocean configuration (NEMO version)		GO4.0 (NEMO 3.4)	GO5.0 (NEMO 3.4)
Coupled configuration		N/A	GC2.0
Atmosphere model resolution		N96	N96
Ocean-ice model resolution		ORCA1	ORCA025
Parameters affecting albedo and radiative forcing (see Sect. 2.2)	α_b	0.61	0.61
	α_C	0.80	0.80
	α_M	0.65	0.72
	T_C	-2.0 °C	-2.0 °C
	T_p	-1.0 °C	-1.0 °C
	$d\alpha/dT$	-0.075 $°C^{-1}$	-0.075 $°C^{-1}$
	f	0.17	0.20
	β	0.4	0.6
Roughness lengths (see Sect. 2.8 of Rae et al., 2014)	z_0(MIZ)	0.0005 m	0.100 m
	z_0(ice)	0.0005 m	0.003 m
Ice salinity (see Sect. 2.7 of Rae et al., 2014)	S	4 ppt	8 ppt
Ridging parameter (see Sect. 2.6 of Rae et al., 2014)	μ_{rdg}	4.0 $m^{1/2}$	3.0 $m^{1/2}$
Thermal conductivities (see Sect. 2.4 of Rae et al., 2014)	κ_{ice}	2.09 W m^{-1} K^{-1}	2.63 W m^{-1} K^{-1}
	κ_{snow}	0.31 W m^{-1} K^{-1}	0.50 W m^{-1} K^{-1}

Table 2. The preprocessor keys used for CICE in GC2.0-GSI6.0

Preprocessor key	Purpose
coupled	Coupled run
ncdf	NetCDF format options available for input and output files
CICE_IN_NEMO	CICE is run in the NEMO environment. CICE is called from the NEMO surface module which also exchanges the coupling fields between NEMO and CICE
ORCA_GRID	Controls reading in grid, land masks and forcing data on the ORCA family of grids.
key_oasis3	Coupling uses OASIS3
REPRODUCIBLE	Ensures global sums bit compare for parallel model runs with different grid decompositions

Table 3. 50-year mean sea ice extent and volume in GSI4.0 and GSI6.0, and equivalent 11-year (1995-2004) means for HadISST and PIOMAS data.

Quantity			GSI4.0	GSI6.0	HadISST	PIOMAS
Sea ice extent (10^6 km^2)	Arctic	Mar	17.68	14.70	15.81	-
		Sept	3.88	7.58	7.23	-
	Antarctic	Sept	19.59	12.67	20.24	-
		Mar	1.43	0.46	5.74	-
Sea ice volume (10^3 km^3)	Arctic	Mar	20.95	27.50	-	26.89
		Sept	1.96	10.81	-	11.56
	Antarctic	Sept	12.12	6.46	-	-
		Mar	0.73	0.11	-	-

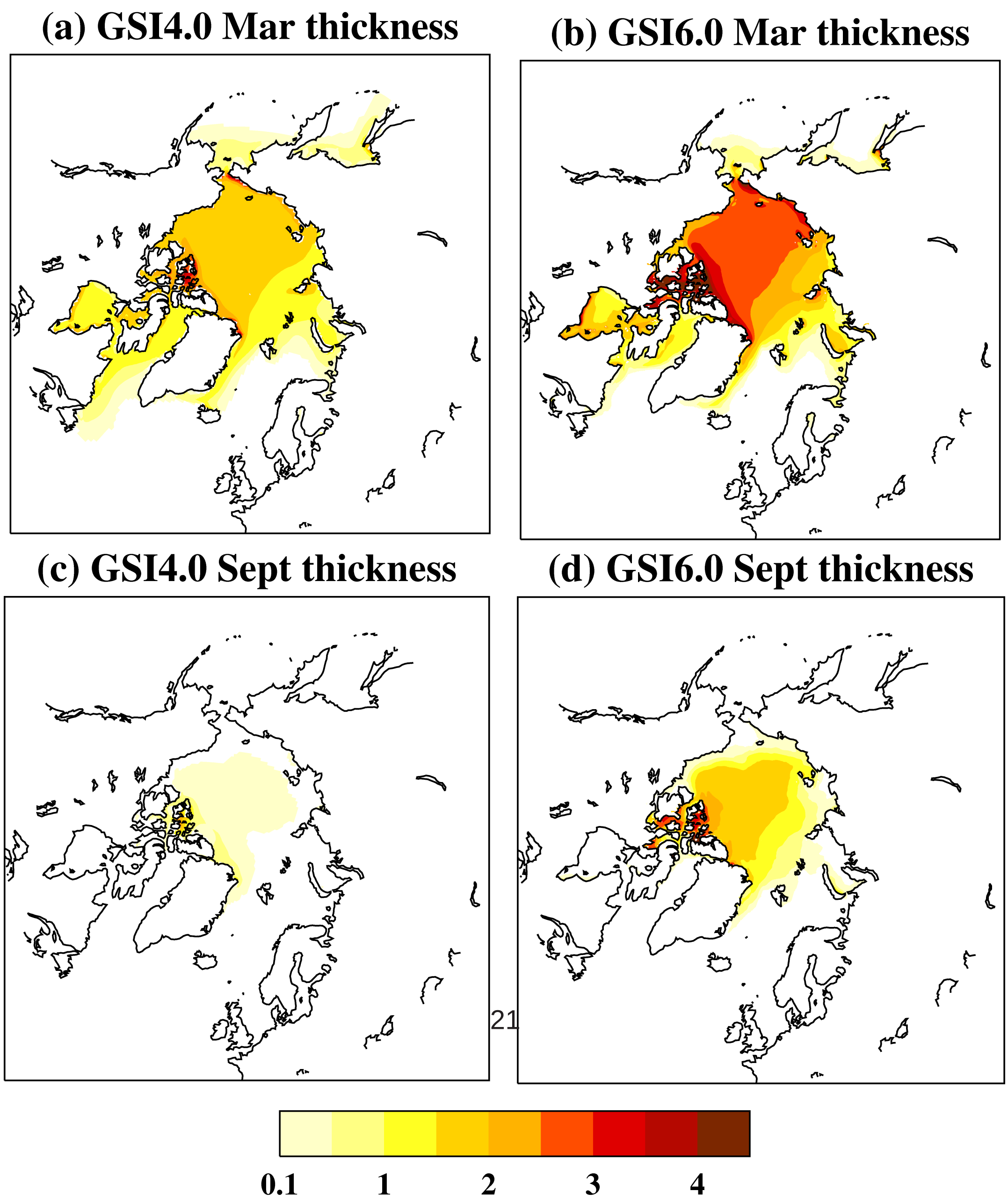

Fig. 1. March and September 50-year mean Arctic sea ice thickness (m) in GSI4.0 and GSI6.0.

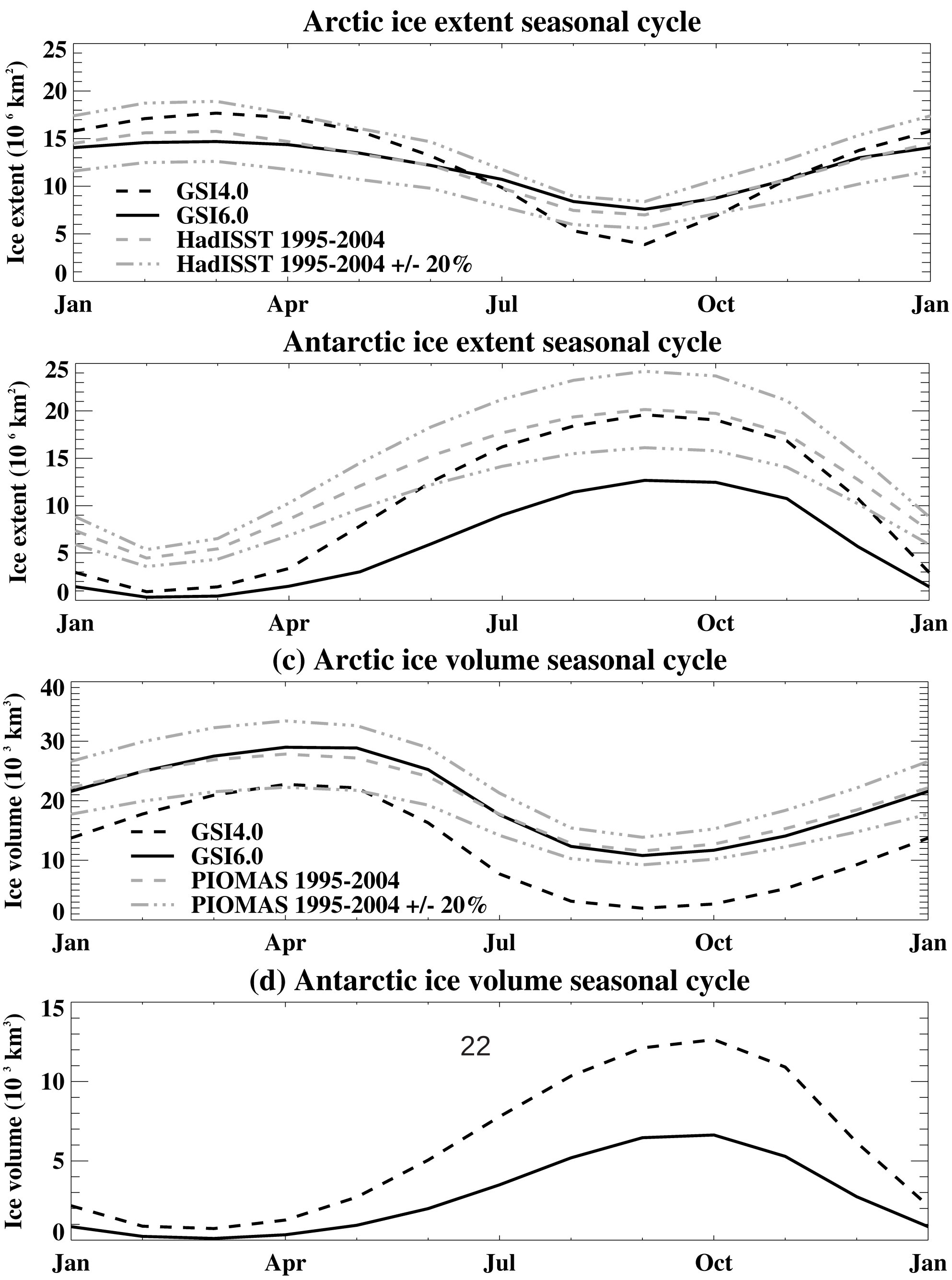

Fig. 2. 50-year mean seasonal cycles of sea ice extent and volume in GSI4.0 and GSI6.0, and equivalent 11-year (1995-2004) mean seasonal cycles for the HadISST and PIOMAS datasets.

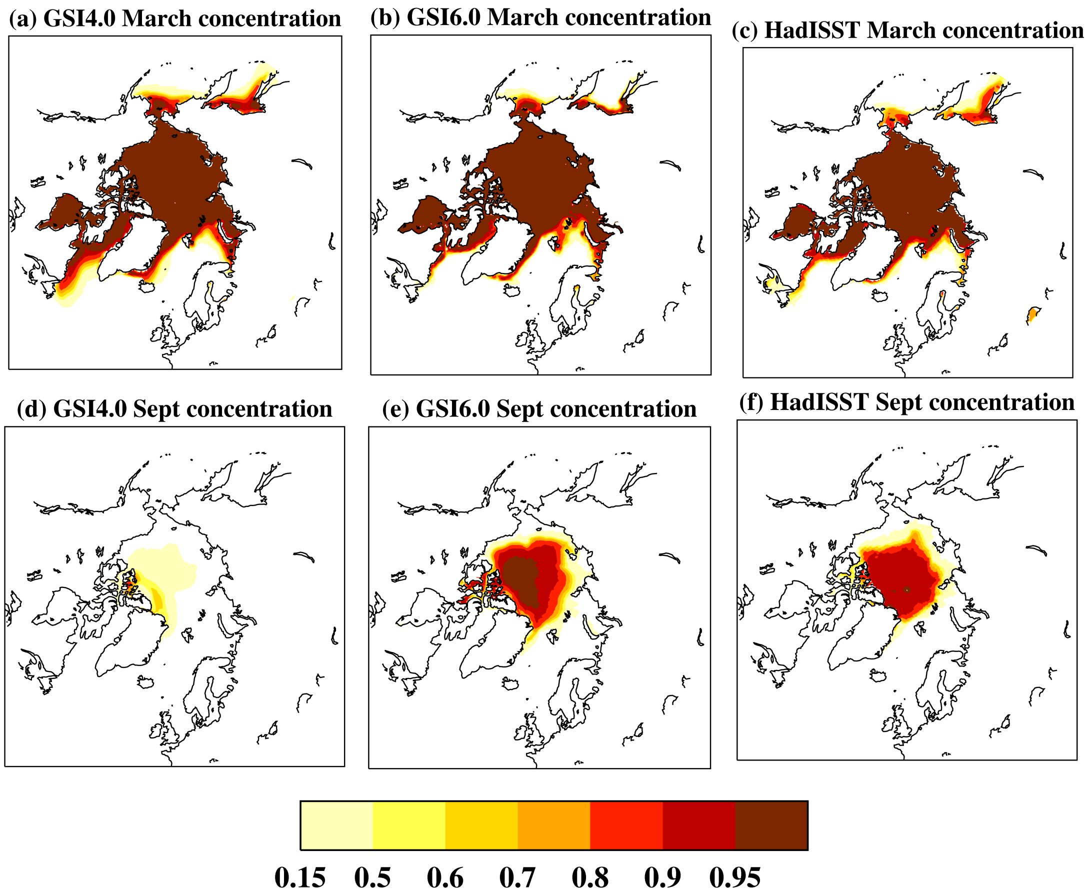

Fig. 3. March and September 50-year mean Arctic sea ice concentration in GSI4.0 and GSI6.0, and equivalent 11-year (1995-2004) means for the HadISST dataset.